

Simple and Double Emulsions via Coaxial Jet Electrospays

Álvaro G. Marín,^{1,*} Ignacio G. Loscertales,² M. Márquez,^{3,4} and A. Barrero^{1,†}

¹Escuela Superior de Ingenieros, Universidad de Sevilla, C. de los Descubrimientos s/n. 41092. Sevilla, Spain

²Escuela Técnica Superior de Ingenieros Industriales, Universidad de Málaga, Málaga, Spain

³Harrington Department Bioengineering, Arizona State University, Tempe, Arizona 85287, USA

⁴Research Center, Philip Morris USA, Richmond, Virginia 23234, USA

(Received 24 April 2006; revised manuscript received 9 July 2006; published 5 January 2007)

We report for the first time the generation of electrified coaxial jets of micrometric diameter in liquid media. Scaling laws to predict the inner and outer diameter of the coaxial jet are given. We show some experiments illustrating the formation process of the coaxial jet, and demonstrate how this process can be used to yield either *o/w* (oil in water) or *o/w/o* (oil/water/oil) emulsions of micrometric size. Some interesting analogies with other hydrodynamic focusing processes are also pointed out.

DOI: [10.1103/PhysRevLett.98.014502](https://doi.org/10.1103/PhysRevLett.98.014502)

PACS numbers: 47.65.-d, 47.15.Uv, 47.55.D-, 47.57.Bc

The interest in the widely known simple and double emulsions is based on the suitability of these liquid-liquid systems to transport substances in a safe and controlled manner. Simple emulsions with dispersed phase in the micrometric range, or especially in the nanometric range, may have applications as antiviral agents, drug delivery, advanced materials, and even in the cosmetics industry [1]. On the other hand, double emulsions permit not only a safer transport of a given substance but also its controlled release.

Among the methods to generate emulsions, classical processes involving bulk processes require long time multistep procedures which generally result in emulsions with wide droplet size distributions. In recent alternative approaches, the liquid interface is smoothly stretched out by the action of either capillary, hydrodynamic, or electrical forces until its characteristic length reaches a critical value (usually in the micro or nanometric range) and the interface breaks by capillary instabilities yielding rather monodisperse drops. These approaches are: (a) dripping or jetting throughout micro-orifices [2], (b) hydrodynamic focusing, i.e., the stretching out of an interface by the high velocity gradients of a converging flow [3], and finally (c) the use of electrohydrodynamic forces for the stretching out of the interface [4]. The two first methods [(a) and (b)] permit a good control of the size of the dispersed phase that can even be extended to the droplet shape by the use of copolymers and induced polymerization [5]. It should be pointed out that in methods of type (a), the distribution of the droplet size is quite narrow; nonetheless, the characteristic cross section of the capillaries (or channels), and therefore, the size of the obtained drops is limited to a few microns to avoid clogging problems. On the other hand, devices based on hydrodynamic focusing (b) are free of the above limitation, although the narrowest size distribution is obtained when the mean size of the droplets is about few tens of microns. Both methods (a) and (b) have been also employed to obtain double emulsions [6], with

good control on both the size of the dispersed phase and the structure of the droplets.

The electrospay technique is one of the few atomizing methods able to reach the submicron scales while still maintaining droplet monodispersity. In ordinary electrospays, a conductive liquid is slowly injected through a needle in an external medium (gas, vacuum, or a dielectric liquid). For appropriate values of the flow rate and the electric voltage applied between the needle and a grounded electrode, the liquid meniscus at the end of the needle adopts a conical shape resulting from the balance between the capillary and the electrohydrodynamic normal stresses [7]. Then, a micrometric (or nanometric) jet issues from the tip of the Taylor cone, which will eventually break up forming a spray (or hydrosol) of charged droplets. In coaxial jet electrospays [8] another liquid is forced through a second needle in such a way that the two liquids coflow to form an electrified coaxial jet; the inner liquid being coated by the outer one. This technique has proved

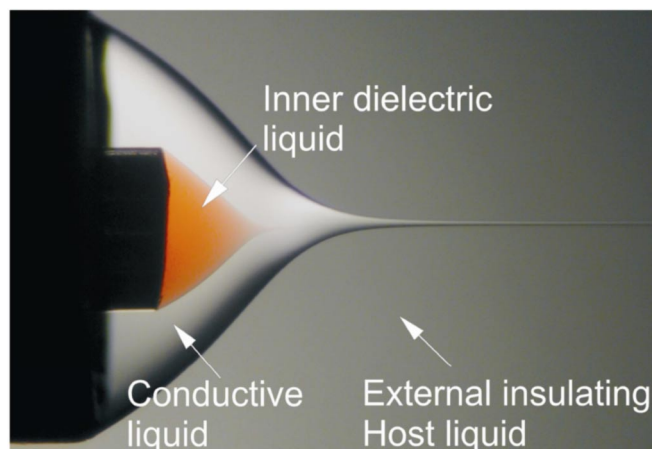


FIG. 1 (color online). Picture of the compound meniscus and the coaxial jets.

its suitability to produce micro and nanoparticles with core-shell structure just in one step (nanocapsules, hollow nanospheres, and both coaxial and hollow nanofibers) [9].

Herein, we report for the first time the stabilization of compound electrospays inside dielectric liquid baths (host liquid). As shown later, either simple (oil in water) or double (oil/water/oil) emulsions can be obtained by this approach. Since the liquids in contact must be immiscible and the host one must be a dielectric, a simple choice to run a compound electrospay within an insulating host would be of the type oil (host)—water (mid)—oil (inner). The configuration is shown in Fig. 1 where the conductive liquid is injected through the annular gap between the needles while the inner insulating one is injected through the inner needle. Once the Taylor cone is formed, the electrical shear stress acting at its interface drags the conductive liquid towards the cone vertex. A steady state jet issues from the vertex when the injected flow rate equals that emitted through the jet. The meniscus at the end of the inner needle is deformed by the converging motion of the conductive liquid. The deformation rate increases with the viscosity of the conductive liquid; therefore, conductive liquids with high viscosity are required for successful operation of compound electrospays in host liquids. For flow rates of the inner liquid higher than a certain minimum, the inner meniscus develops a steady state spout that evolves into a jet which flows coaxially with the conductive liquid jet (Fig. 1). For values of the inner flow rate below the minimum one, the inner liquid seems to be emitted in a periodic dripping mode. Obviously, another steady state is found when no inner liquid is injected. In this case, the drop tip presents a hump whose curvature increases with the deformation rate. Extremely sharp tips can be developed if the interfacial tension is sufficiently large to support the deformation, as in the case shown in Fig. 2, where the curvature radius has an approximate value of $4 \mu\text{m}$. These conical points remain steady for times of order of hours with no detectable loss of mass by neither dripping nor jetting. Note that the emission of mass of the inner liquid would require capillary numbers, $\mu_e U / \gamma_i$, of order unity (shear stress overcoming surface tension) and therefore the emitted flow rate would be $Q_i \sim UR^2 \sim \gamma_i R^2 / \mu_e$, which is of order of nanoliters per second for

typical values of the interfacial tension γ_i , viscosity of the conductive liquid μ_e , radius of curvature at the apex R , and for the liquid velocity $U \sim \gamma_i / \mu_e$. Since the volume of the inner liquid meniscus is of the order of nanoliters (needle diameter ranging from 40 to 100 microns) any emission of mass from the meniscus would be detected for such flow rates in times of order of seconds.

The transition from a conical point to a steady jet, which occurs when the inner flow rate increases above a minimum one, is depicted in the set of consecutive pictures in Fig. 2. As the drop volume increases, the drop tip moves towards the vertex of the Taylor cone where deforming velocities are higher; consequently, the radius of curvature of the tip decreases until a minimum cutoff is reached and a spout develops. The key role of the capillary tension at the tip meniscus is illustrated in the experiment reported in Ref. [10]. It is worthy to point out that the formation of the inner jet described above resembles other related topological transition phenomena like those driven either by mechanical stresses (selective withdrawal and other viscous liquid entrainments [3]) or by electrical stresses [11]. At flow rates near the minimum one, we have observed that instead of a clear transition from jetting to dripping, the jet undergoes a sequence of small oscillations in its diameter until the meniscus retracts after emitting a liquid thread or a train of small droplets. The time scale for this oscillation is rather long (of order of minutes) and the measurements of the jet diameter are imprecise due to its narrowness (of order of a few microns); therefore, it is difficult to identify the threshold flow rate of the jet instability. In addition, at these scales, the visualization of the inner meniscus is blurred by the presence of the external charged interface, even with high quality optical equipment. Thus, precise measurements of the transition threshold will require more advanced techniques.

Measurements of the diameters of the inner and the outer jets have been carried out by direct observation through an optical system. Special care has been taken to make sure that only steady state jets were considered in our measurements. In these series of experiments, glycerol, several silicone oils (with viscosities varying along 3 orders of magnitude), and hexane have been used, respectively, as conductive, inner, and host liquids (see Ref. [12]). It should be noticed that the presence of a host liquid surrounding the compound meniscus allows sharper observation of the inner jet. Certainly, reflection of light on liquid-liquid interfaces is weaker than those on liquid-air interfaces (the reason is found in the refractive index difference), and this permitted us to observe clearly inside the jets. Nonetheless, the measurements of the diameter of the inner jet need to be corrected to account for the refraction of light at the glycerine-hexane interface (a correction of 7% in the observed diameter is included for the glycerine-hexane interface). In Fig. 3(b) we present the resulting inner-to-outer jet diameter ratio versus inner-to-outer

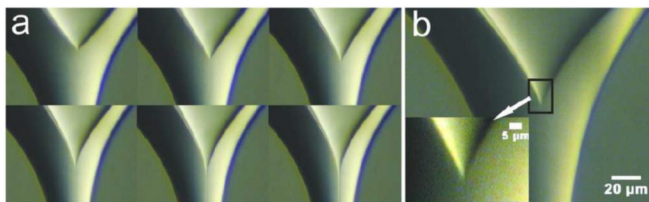


FIG. 2 (color online). (a) Transition of the inner meniscus from steady conical meniscus to jet mode as the injected flow rate is increased (from left to right) above its minimum. (b) Unsteady spout slightly below minimum flow rate.

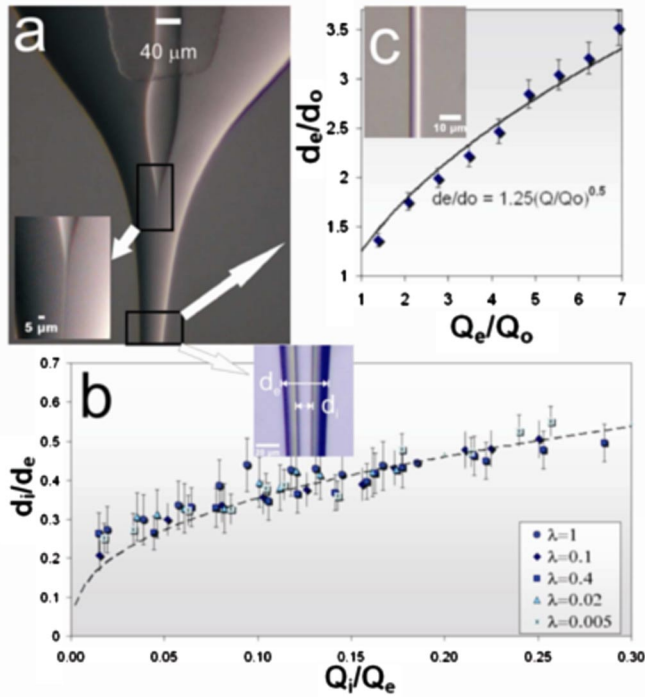


FIG. 3 (color online). (a) Image of the coaxial jet electrospray employed for the experiment: pure glycerol is used as external conductive liquid while silicone oil (with viscosity 20 cSt) is being issued from the inner silica capillary needle. (b) Measurements of the external charged jet diameter vs its injected flow rate are also plotted. (c) Measurements of inner-to-outer jet diameter ratio vs inner-to-outer flow rate ratio.

flow rate ratio, for five different inner liquids and just one outer liquid. It is worth mentioning that for a given flow rate ratio, the differences in the jet diameter ratio for the different liquids are of the same order than the experimental error. Therefore, within this experimental error, one can conclude that the jet diameter ratio is practically independent of the viscosity of the inner liquid. Note that the Reynolds number $R_e \sim \rho_i Q_i / \mu_i d_i$ of the flow in the inner jet is of order unity even in the case of the liquid with the smallest viscosity (typical values of Q_i and d_i in the experiment are, respectively, 40 nl/s and 10 μm). Therefore, the velocity profile of the inner liquid is relaxed (i.e., the profile becomes almost flat) within jet lengths of several diameters. Then, one would expect a behavior for the diameter ratio of the type $d_i/d_e \sim (aQ_i/Q_e)^{1/2}(1 + aQ_i/Q_e)^{-1/2}$, where factor a , which is larger than 1, accounts for the fact that the average velocity of the outer liquid is larger than the velocity of the inner liquid, and subscripts i and e indicate inner and outer liquids, respectively. Note that for $a = 1.4$, the theoretical law behavior agrees quite well with the experimental results. Nonetheless, simple calculations show that assumption $a = 1$ underestimates the diameter ratio by only 12% in the worst case. In addition, the above semiempirical scaling law allows for the prediction of the diameter ratio of the electrified coaxial jet issued from compound electrosprays

inside liquid baths. Note also from Fig. 3(b) that the lowest values of Q_i for the five liquids, which have been measured at constant Q_e are practically equal in spite of $\lambda = \mu_i/\mu_e$ spans over 3 orders of magnitude. In addition, as reported recently [13], the maximum curvature of the steady conical meniscus and its conical angle neither depend on the viscosity of the inner liquid. These facts resemble the behavior of the steady humps reported in selective withdrawal and other similar entrainment experiments [3], in which a liquid is withdrawn through a tube placed above a liquid-liquid interface at certain distance producing a hump on the lower liquid whose curvature increases with the suction flow rate; when a critical value of the flow rate is reached the hump transforms into a jet. Both the critical straw height and the critical meniscus curvature have been found to be independent of the viscosity of the lower liquid (at least for viscosity ratios $\mu_{\text{upper}}/\mu_{\text{lower}} > 1$). In fact, they only depend on a capillary number based on interfacial tension and on external shear stress; this behavior is very similar to that observed in our experiment.

Figure 3(c) shows the diameter of the outer liquid jet as a function of its flow rate. Since the outer liquid is being electrosprayed in the so-called cone-jet mode [14], we use the characteristic jet diameter, $d_o = (\epsilon_o^2 \gamma_e \rho_e K^2)^{1/3}$, and characteristic flow rate, $Q_o = \epsilon_o \gamma_e / \rho_e K$, given in classical electrospray literature [15]; ϵ_o , γ_e , K , and ρ_e are, respectively, vacuum permittivity, surface tension, electrical conductivity, and density of the liquid. Results fit a law of the form $d_e/d_o = 1.25(Q_e/Q_o)^{1/2}$ which is in quite good agreement with previously reported measurements of droplet sizes in electrosprays [4,15].

Because of capillary instabilities, the coaxial jet breaks up at some point downstream giving rise to compound droplets [Figs. 4(a) and 4(b)]. Note that to obtain sharp pictures of the capsule structures using optical microscopy, the size of the capsules must be sufficiently large, which requires high flow rates. Unfortunately, the best degree of polydispersion in the mean size of the droplets is obtained for the lowest jet diameters (lower values of the flow rate), for which visualization of the droplets is much harder. Different capsule structures can be obtained by appropriate tuning of both flow rates. Capsules with several small nuclei are obtained when the outer to inner flow rate ratio is high enough [50 to 1 as in the case in Fig. 4(a)]; as expected, the number of nuclei can be reduced to one either by reducing the outer flow rate or by increasing the inner one [flow rate ratio 5 to 1 as in the case in Fig. 4(b)].

Water in oil (*w/o*) emulsions can be generated by simple electrosprays in dielectric liquid baths as reported in [4], but never oil in water emulsions. However, *o/w* emulsions can be obtained by using compound electrosprays inside a dielectric liquid host. Indeed, let us consider a denser water phase connected to a grounded electrode below the lighter host liquid (hexane in this case). Capsules generated from a the breakup of an electrified coaxial jet consisting of a dielectric liquid coated by a conductive one (an oil/water

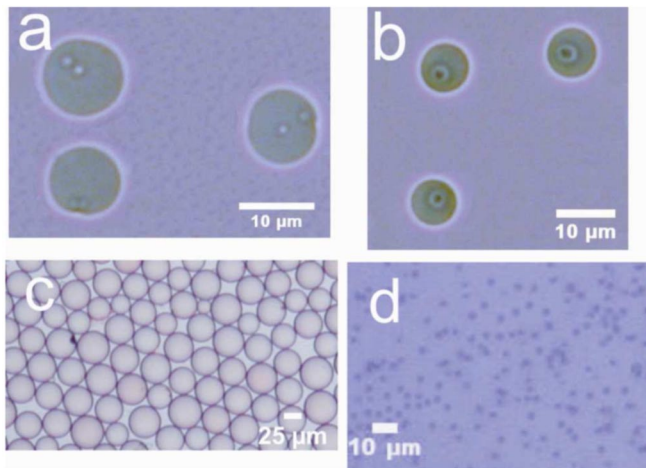


FIG. 4 (color online). (a) In the capsules shown in the image, a high external-to-inner flow ratio gives rise to relatively big capsules containing several small nuclei ($\leq 1 \mu\text{m}$). (b) By reducing flow rate ratio only one nucleus is placed in the capsules. (c) Simple droplets of carbon tetrachloride (Cl_4C) in a water based polymeric solution; for easier visualization we have employed higher flow rates yielding large droplets. (d) Smaller particles ($< 2 \mu\text{m}$) of Vaseline oil in water with narrower size distribution can also be easily obtained.

capsule) move towards the grounded water phase under the action of both the electric field and gravity. Once the capsules reach the water phase, the shell dissolves and the oil is released into the water phase forming the oil/water emulsion [Fig. 4(c) and 4(d)].

The electrospray technique has proved its capability to generate droplets with diameters down to the submicrometric range if the conductivity of the liquid is enhanced up to sufficiently high values. On the other hand, particle size distributions are broader than those obtained by other methods reported in the literature. Nonetheless, it has been also proved that operation of the electrosprays at flow rates not far from the minimum one substantially narrows the size distribution of the obtained capsules. Additionally, the shell thickness of core-shell capsules and its size can be estimated as a function of the flow rate ratio from the expressions for the inner and outer diameters of the jet.

A. G. Marin would like to thank Mr. M. Gonzalez for its technical assistance with the experiments in the laboratory and Dr. J. M. Gordillo for helpful discussions on the subject. This work has been supported by the Spanish Ministry of Education and Science under Project No. BFM2001-

3860-C02-01 and also No. DPI2004-05246-C04-01.

*Email address: alvarogm@us.es

Electronic address: <http://eurus2.us.es>

†Email address: abarrero@us.es

- [1] T. Hamouda *et al.*, *J. Appl. Microbiol.* **89**, 397 (2000); J. M. Odeberg *et al.*, *European Journal of Pharmaceutical Sciences* **20**, 375 (2003); A. Fernández-Nieves *et al.*, *Adv. Mater.* **17**, 680 (2005); O. Sonnevile-Aubrun *et al.*, *Adv. Colloid Interface Sci.* **108**, 145 (2004).
- [2] H. Willaime *et al.*, *Phys. Rev. Lett.* **96**, 054501 (2006).
- [3] L. Martin-Banderas *et al.*, *Adv. Mater.* **18**, 559 (2006); S. L. Anna *et al.*, *Appl. Phys. Lett.* **82**, 364 (2003); I. Cohen *et al.*, *Science* **292**, 265 (2001); I. Cohen and S. R. Nagel, *Phys. Rev. Lett.* **88**, 074501 (2002); W. W. Zhang, *Phys. Rev. Lett.* **93**, 184502 (2004); S. C. du Pont and J. Eggers, *Phys. Rev. Lett.* **96**, 034501 (2006).
- [4] A. Barrero *et al.*, *J. Colloid Interface Sci.* **272**, 104 (2004).
- [5] S. Xu *et al.*, *Angew. Chem., Int. Ed. Engl., Suppl.* **44**, 3799 (2005).
- [6] A. S. Utada *et al.*, *Science* **308**, 537 (2005).
- [7] G. I. Taylor, *Proc. R. Soc. A* **280**, 383 (1964).
- [8] I. G. Loscertales *et al.*, *Science* **295**, 1695 (2002).
- [9] I. G. Loscertales *et al.*, *J. Am. Chem. Soc.* **125**, 1154 (2003); I. G. Loscertales *et al.*, *J. Am. Chem. Soc.* **126**, 5376 (2004); J. Xia and Y. Hsieh, *J. Mater. Sci.* **38**, 2125 (2003).
- [10] A film of one of these experiments can be watched in “Gouttes, bulles, perles et ondes. Avec 200 expériences filmées,” P. de Gennes, F. Brochard-Wyart, and D. Quere, Berlin, 2005; see EPAPS Document No. E-PRLTAO-98-036702 for other videos on the subject. For more information on EPAPS, see <http://www.aip.org/pubservs/epaps.html>.
- [11] L. Oddershede and S. R. Nagel, *Phys. Rev. Lett.* **85**, 1234 (2000).
- [12] See EPAPS Document No. E-PRLTAO-98-036702 for the liquid properties and setup details. For more information on EPAPS, see <http://www.aip.org/pubservs/epaps.html>.
- [13] A. G. Marin *et al.*, *58th Annual Meeting of the Division of Fluid Dynamics*, Bull. Am. Phys. Soc. Report No. NB-5, p. 197, 2005.
- [14] M. Cloupeau and B. Prunet-Foch, *J. Electrostat.* **22**, 135 (1989).
- [15] A. M. Gañan-Calvo, J. Davila, and A. Barrero, *J. Aerosol Sci.* **28**, 2 (1997); J. F. de la Mora *et al.*, *J. Aerosol Sci.* **21**, 169 (1990); J. Rosell-Llompart and J. Fernandez de la Mora, *J. Aerosol Sci.* **25**, 1093 (1994).